Available online at www.sciencedirect.com
ScienceDirect
Advances in Space Research 41 (2008) 2043–2049
ADVANCES IN SPACE RESEARCH (a COSPAR publication)
www.elsevier.com/locate/asr

The PAMELA experiment: A space-borne observatory for heliospheric phenomena

M. Casolino *, P. Picozza, On Behalf of the PAMELA collaboration

INFN, Structure of Rome Tor Vergata, Physics Department, University of Rome "Tor Vergata", I-00133 Rome, Italy

Received 11 November 2006; received in revised form 21 May 2007; accepted 23 June 2007

Abstract

PAMELA is a multi-purpose apparatus composed of a series of scintillator counters arranged at the extremities of a permanent magnet spectrometer to provide charge, time-of-flight and rigidity information. Lepton/hadron identification is performed by a silicon–tungsten calorimeter and a Neutron detector placed at the bottom of the device. An Anticounter system is used offline to reject false triggers coming from the satellite. The device was put into orbit on June 15th 2006 in a pressurized container on board the Russian Resurs-DK1 satellite. The satellite is flying along a high inclination (70°), low Earth orbit (350–600 km), allowing to perform measurements in different points and conditions of the geomagnetosphere. PAMELA main goal is a precise measurement of the antimatter ($\bar{p}$ 80 MeV–190 GeV, e^+ 50 MeV–270 GeV) and matter (p 80–700 GeV, e^- 50 MeV–400 GeV) component of the galactic cosmic rays. In this paper we focus on the capabilites of observations of heliospheric cosmic rays: trapped and semi-trapped particles in the proton and electron belts, solar particle events, Jovian electrons will be studied in the three years of expected mission.

Keywords: Cosmic rays; Satellite-borne experiment; Solar wind; Solar energetic particles; Jovian particles

1. Overview

The PAMELA experiment is a satellite-borne apparatus devoted to the study of cosmic rays, with an emphasis on its antiparticle component. The device is constituted by a number of highly redundant detectors capable of identifying particles providing charge, mass, rigidity and beta information over a very wide energy range (Picozza et al., 2007; Casolino et al., in press). The instrument is built around a permanent magnet (Adriani et al., 2002) with a microstrip tracker (six double sided planes) providing rigidity and sign of charge information. A scintillator system (six layers arranged in three planes for a total of 48 phototubes) is used to provide trigger, charge and time-of-flight information (Barbarino et al., 2003). Hadron/lepton separation is performed with a 44 plane silicon–tungsten calorimeter (Boezio et al., 2002) (16.3 radiation lengths, 0.6 interaction lengths). A shower tail catcher and a neutron detector (Galper, 2001) at the bottom of the apparatus increase this separation. An Anticounter system (Orsi et al., 2006) is used to reject spurious events in the offline phase. Around the detectors are housed the readout electronics, the interfaces with the CPU (Casolino et al., 2006) and all primary and secondary power supplies. The system is enclosed in a pressurized container located on one side of the Resurs-DK satellite (see Fig. 1). Total weight of PAMELA is 470 kg; power consumption is 355 W, geometrical factor is 21.5 cm^2 sr. The detector is capable of identifying protons (in the energy range 80 MeV–700 GeV), electrons (50 MeV–400 GeV), antiprotons (80 MeV–190 GeV), positrons (50 MeV–270 GeV) and nuclei up to $Z = 8$ up to $\simeq$100 GeV. The launch occurred on June the 15th 2006 from the cosmodrome of Baikonur with a Soyuz rocket. The satellite flies on a quasi-polar (inclination 70°), elliptical (altitude 350–600 km) orbit with an expected mission duration of three years. The orbit, the long observational lifetime, and the structure of the detector allow PAMELA

* Corresponding author.
E-mail address: Marco.Casolino@roma2.infn.it (M. Casolino).

0273-1177/$34.00 © 2008 Published by Elsevier Ltd on behalf of COSPAR.
doi:10.1016/j.asr.2007.06.061

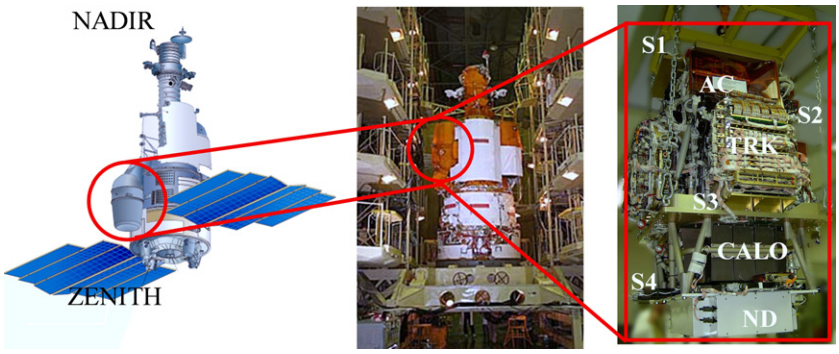

Fig. 1. Left: Scheme of the Resurs-Dk1 satellite. PAMELA is located in the pressurized container on the left of the picture. In the scheme the pressurized container is in the acquisition configuration. Center: The Resurs-DK satellite during integration in Samara. The pressurized container housing Pamela is in the folded (launch) position. Right: Photo of the PAMELA detector in Tor Vergata with marked the position of the detectors. S1, S2, S3, S4: scintillator planes; AC: top anticoincidence; TRK: tracker core; CALO: silicon–tungsten calorimeter; ND: neutron detector.

to address several items in cosmic-ray physics, increasing knowledge of cosmic-ray origin and propagation. Also cosmological issues related to detection of a dark matter signature and search for antimatter (PAMELA will search for $\overline{\text{He}}$ with a sensitivity of $\approx 10^{-8}$) will therefore be addressed with this device. In this work we focus on the scientific objectives and observational capabilities for PAMELA to detect detection of the solar and heliospheric cosmic rays.

2. In flight data

A typical behaviour of the acquisition of PAMELA is shown in Fig. 2. The three plots show the counting rate of the three scintillator planes and are sensitive to particles of increasing energy. Highest rate (black) represents the counting of the top scintillator plane (S11 * S12), triggered by $E \geqslant 36$ MeV protons and $E \geqslant 2.5$ MeV e^-. Middle plot (red in the online version) shows the particle rate measured by the coincidence of the middle planes, above the tracker (S21 * S22), which requires protons and electrons of at least 63 and 9.5 MeV respectively. The bottom layers, located below the tracker (S31 * S32) exhibit the smallest rate (blue in online version), which is triggered by protons and electrons of energy above 80 and 50 MeV entering from the top (lower energy particles may penetrate the detector from the sides and increase the counting rate). The different thresholds are evident in the counting rate of the scintillators: for instance the first SAA passage, corresponding to the easternmost passage is highest in S1 and absent in the S3 counting rate. The following passages occur closer to the center of the SAA and saturate several times the ADC counting rate of the S1 scintillator but not the other two scintillators. This is consistent with the power law spectrum of trapped particles in the SAA and the geometrical size of the two scintillators. Also S2 and S3 counting rate ratio in the anomaly is about 5, consistent with a particle flux ratio evaluated with AP8 algorithm (Gaffey and Bilitza, 1994). Outside the SAA it is possible to see the increase of particle rate at the geomagnetic poles due

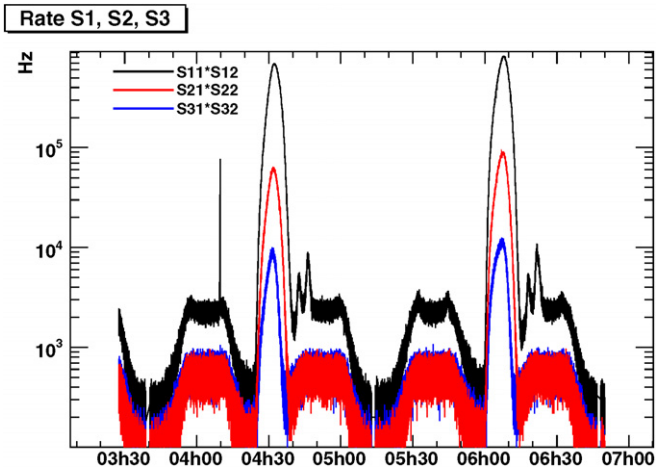

Fig. 2. Counting rates of PAMELA scintillators: top (S1 – black), center (S2 – red), bottom (S3 – blue) as a function of time (see text). (For interpretation of color mentioned in this figure legend the reader is referred to the web version of the article.)

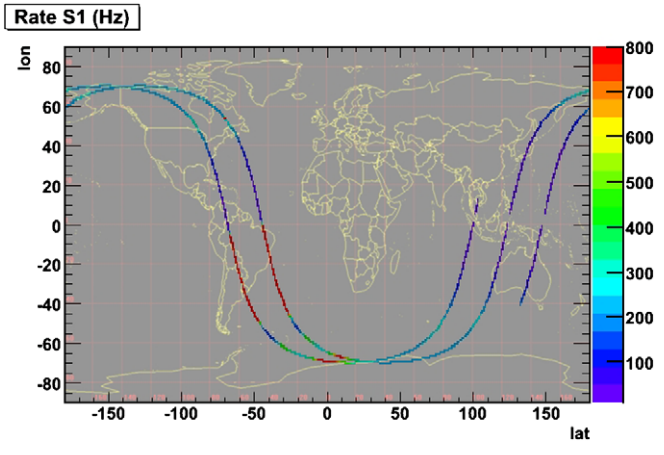

Fig. 3. Ground track of PAMELA with counting rate of the main trigger configuration ((S11 + S12) * (S21 + S22) * (S31 + S33)) corresponding to $E \geqslant 50$ MeV e^- and $E \geqslant 80$ MeV p. Note the particle rate increase in the South Atlantic Region, where the proton belt is crossed and in the polar regions where cutoff is lower.

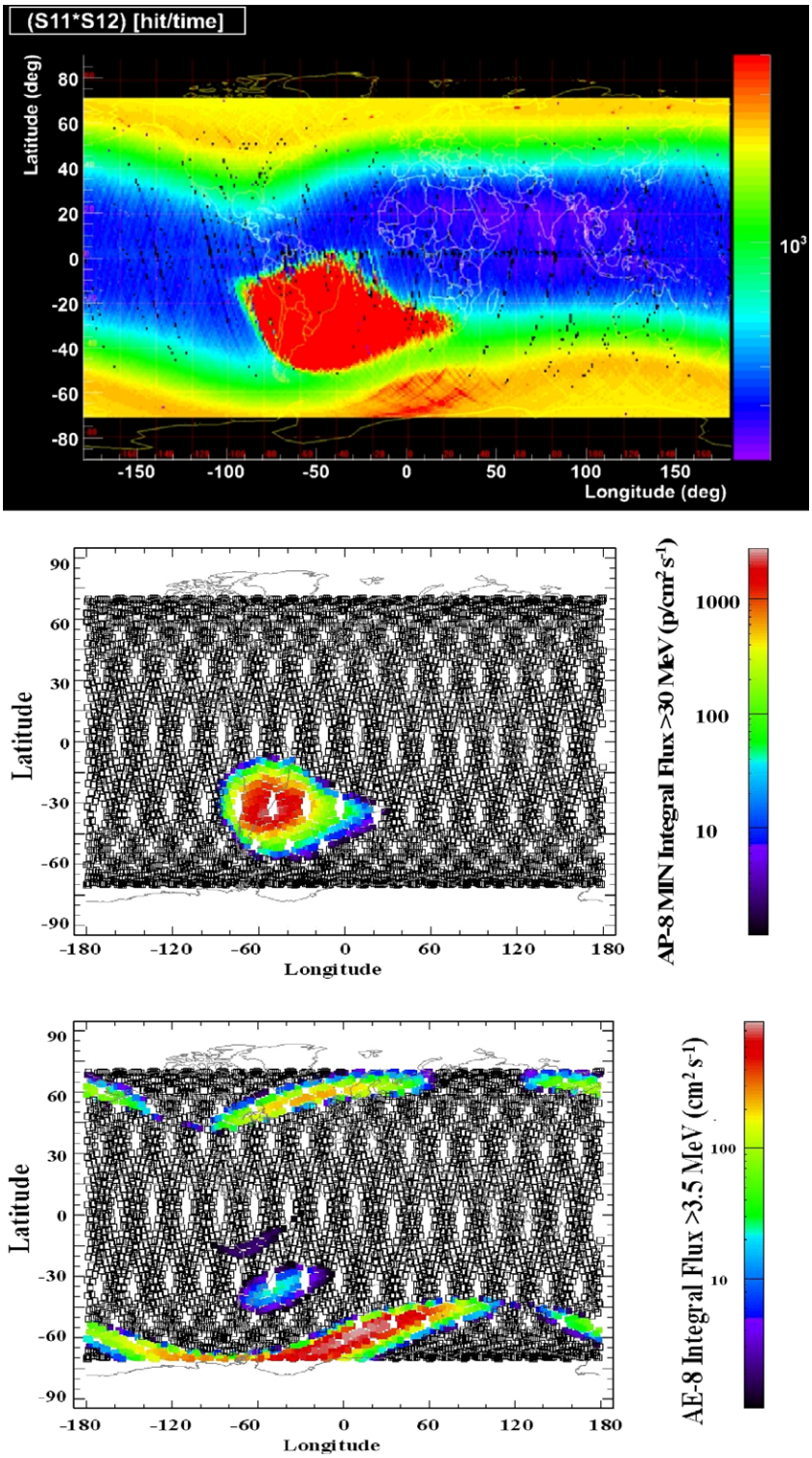

Fig. 4. Top panel: Counting rate of S11 * S12 (p 36 MeV, e^- 2.5 MeV). Center panel: Flux rate from AP-8 Model (integral flux above 30 MeV). Bottom panel: Flux rate from AE-8 Model (integral flux above 3.5 MeV).

to the lower geomagnetic cutoff. The highest rates are found when the satellite crosses the trapped components of the Van Allen Belts. In Fig. 3 it is possible to see the main trigger rate as a function of the ground track of PAMELA. The pause in the acquisition at the equator is due to the calibration of the subdetectors usually performed during the ascending phase to avoid crossing the radiation belts.

3. Trapped particles

Protons with $E \geqslant 80$ MeV cross all three scintillator planes and the tracker of PAMELA allowing a precise determination of the energy spectrum of the high energy component of the trapped proton belt. Data will be used to validate existing models and to extend their validity to higher energies. Also the stability of the belts and the long and short term temporal fluctuations will be analyzed. PAMELA can also perform measurements at lower energies using the counting rate of the scintillators using the range method. In this way it is possible to extend the range of PAMELA performing integral proton flux measurements from 36 MeV and electron flux from 3.5 MeV. This threshold is determined by the minimum energy required to cross the Aluminum of the pressurized container and release a signal in S11 and S12. Other trigger configurations (requiring crossing of S2 scintillator) will allow to measure integral spectra with higher flux. In Fig. 4 it is possible – for instance – to see PAMELA world particle rate for S11 * S12 counter, showing the high latitude electron radiation belts and the proton belt in the South Atlantic Anomaly. Note that counting rate in the northern electron belt is less intense than the southern because PAMELA orbit height is $\simeq$350 km in that region as compared to the $\simeq$600 km in the South. In the other panels are shown the simulations obtained with AP-8 and AE-8 models using (Spenvis) environment on the same orbit of PAMELA which show a good agreement between data and simulation.

4. Solar energetic particles

The launch of PAMELA took place during solar minimum and data taking will be performed for at least three years in the recovery phase going toward solar maximum of cycle 24. The number of expected solar proton events in the three years of mission can be estimated from Shea and Smart (2001): we expect about 10 solar events with $E > 80$ MeV (necessary to trigger the apparatus) in the three years of the nominal experiment lifetime. Events with fluence at lower energy can be observed using the already mentioned technique of scintillator counting. In case of large events the rate of background particles hitting the top scintillator (S1) could be very high for intense solar events: therefore a different trigger configuration (e.g. using only S2 and S3) has to be set in these cases.[1] The observation of solar energetic particle (SEP) events with a magnetic spectrometer will allow several aspects of solar and heliospheric cosmic-ray physics to be addressed for the first time.

4.1. Protons

PAMELA is able to measure the solar component over a very wide energy range (where the upper limit will be limited by statistics and therefore the size of the event and its spectral characteristics). Up to now there has been no direct measurement (Miroshnichenko, 2001) of the high energy (>1 GeV) proton component of SEPs. The importance of a direct measurement of this spectrum is related to the fact (Ryan, 2000) that there are many solar events where the energy of protons is above the highest ($\simeq$100 MeV) detectable energy range of current spacecrafts, but is below the detection threshold of ground Neutron Monitors (Bazilevskaya and Svirzhevskaya, 1998). With PAMELA it will be possible to examine the turnover of the spectrum, where the limit of acceleration processes at the Sun is reached. Our instrument has a maximum trigger rate of about 60 Hz and a geometrical factor of 21.5 cm^2 sr. This implies that we will be able to read all events with an integral flux (above 80 MeV) up to 4 particles/(cm^2 s sr). For such events we expect about 2×10^6 particles/day (assuming a spectral index of $\gamma = 3$ we have 2×10^3 events/day above 1 GeV). Larger events will saturate the trigger, so in this case the number of protons will be reduced by dead time and mass memory limitations.

4.2. Positrons

Positrons are produced mainly in the decay of π^+ coming from nuclear reactions occurring at the flare site. Up to now, they have only been measured indirectly by remote sensing of the gamma ray annihilation line at 511 keV. Using the magnetic spectrometer of PAMELA it will be possible to separately analyze the high energy tail of the positron spectra obtaining information both on particle production and charge dependent propagation in the heliosphere through comparison of the temporal and energetic profile of the e^- and e^+ flux.

4.3. Nuclei

PAMELA can identify light nuclei up to Oxygen and isotopes of Hydrogen and Helium. Thus it is possible to investigate the light nuclear component related to SEP events over a wide energy range. Applying the same estimates as above, we can expect $\simeq 10^4$ ^{4}He and $\simeq 10^2$ ^{3}He nuclei for gradual events, and more for impulsive ones. Such a high statistics will allow us to examine in detail the amount of the ^{3}He and deuterium up to 3 GeV/c. This should contribute to establish whether there are differences in the composition of the high energy (1 GeV) ions to the low energy component ($\simeq$20 MeV) producing γ rays or the quiescent solar corona (Ryan, 2005) and better understand the

[1] This can be performed automatically by the on board CPU in case of high counting rate of the top scintillator or by specific ground command, using information coming from the satellite monitoring system (e.g. SOHO, ACE, GOES). In this way observation and memory filling would therefore vary according to the event type (impulsive, gradual) and intensity.

selective acceleration processes in the higher energy impulsive (Reames, 1999) events.

4.4. Neutrons

Neutrons are produced in nuclear reactions at the flare site and can reach the Earth before decaying (Chupp et al., 1982). Although there is no devoted trigger for neutrons in PAMELA, the background counting of the neutron detector will measure in great detail the temporal profile and distribution of solar neutrons. In Fig. 5 is shown the acquisition of neutrons vs time for the two neutron detector layers. It is possible to see how the rate depends on the geomagnetic cutoff, being higher at high latitudes and lower at the equator. During crossing of the South Atlantic Anomaly neutron flux increases considerably. Measured rate drops to zero three times during calibrations. The background counting system keeps track of the number of neutrons which hit the neutron detector in the time elapsed since last trigger. The counter is reset each time it is read allowing for a precise measurement of background neutron conditions during the mission. On the occurrence of solar events, neutrons are expected to reach Earth before protons as they have no charge. They are not deflected by any magnetic field and will be directly recorded by PAMELA (if it is not in Earth's shadow) increasing counts over the expected background.

4.5. Lowering of the geomagnetic cutoff

The high inclination of the orbit of the Resurs satellite will allow PAMELA to study the variations of cosmic-ray geomagnetic cutoff due to the interaction of the SEP events with the geomagnetic field (Ogliore et al., 2001; Leske et al., 2001).

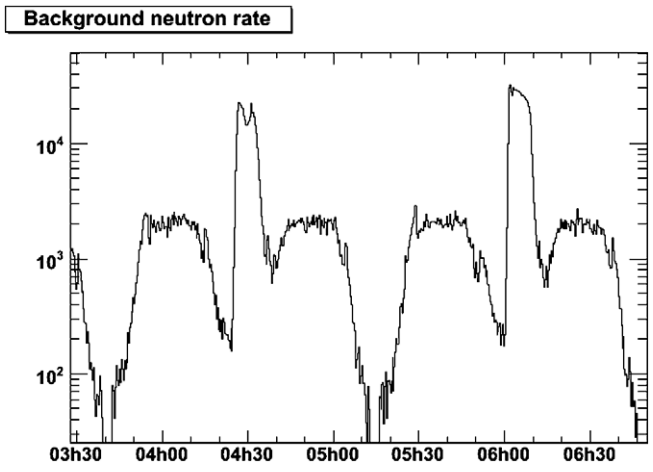

Fig. 5. Counting rate (n/min) for the neutron detector averaged on the two layers of ^{3}He tubes. The graph refers to the same period of Figs. 2 and 3. It is possible to see the rate oscillation due to different particle cutoff (lower at the equator and higher at the poles) and the increase when crossing the SAA.

5. Jovian electrons

Since the discovery made by Pioneer 10 of Jovian electrons at about 1 AU from Jupiter (Simpson et al., 1974; Eraker, 1982), with an energy between 1 and 25 MeV, several interplanetary missions have measured this component of cosmic rays. At 1 AU from the Sun the IMP-8 satellite could detect Jovian electrons in the range between 0.6 and 16 MeV and measure their modulation by the passage of Coronal Interaction Regions (CIR) with 27 days periodicity (Eraker, 1982; Chenette, 1980). There are also long term modulation effects related to the Earth–Jupiter synodic year of 13 months duration. Since Jovian electrons follow the interplanetary magnetic field lines, when the two planets are on the same solar wind spiral line, the electron transit from Jupiter to the Earth is eased and the flux increases. When the two planets lie on different spiral lines the electron flux decreases. Currently we know that Jupiter is the strongest electron source at low energies (below 25 MeV) in the heliosphere within a radius of 11 AUs from the Sun. Its spectrum has a power law with spectral index $\gamma = 1.65$ up to 70 MeV, where the galactic component becomes dominant. Many models attempt to describe the complex processes of Jovian and galactic electron diffusion in the solar wind. For instance in Chenette (1980) a convection diffusion model is used applying the results to IMP8 and Pioneer 10 and 11 data. More recently Ferreira et al. (2001) and Ferreira (2005) developed a three dimensional model with convection, gradient and curvature drift and current sheet effects. Measurements in the energy range 50–130 MeV at 1 AU will contribute to test the validity of these models at high energies and in the recovery period from solar minimum.

In addition to the primary component, Jovian electrons can reach the Solar Wind Termination Shock (TS) and be accelerated. It is known that cosmic rays originating outside the heliosphere can be accelerated at the solar wind TS. This applies also to Jovian electrons, which are transported outward by the solar wind, reach the TS and undergo shock acceleration thus increasing their energy. Some of these electrons are scattered back in the heliosphere and reach 1 AU. Reacceleration intensity and spectral feature depends upon shock position (Poitgieter and Ferreira, 2002): a precise measure of the high energy component and its modulation with synodic year could also contribute to determine the overall characteristics of the shock. Electrons can be detected by PAMELA in the energy range between 50 MeV and 400 GeV measuring their energy with the magnetic spectrometer. The spectrometer allows also separation and identification of the positron component in the 50 MeV–290 GeV range. The electron spectrum been measured at 1 AU by several space-borne such as OGO-V (L'Heureux and Meyer, 1976) – $\simeq$10 – 200 MeV and balloon-borne experiments (e.g. Evenson et al., 1983; Boezio et al., 2000, above $\simeq$30 GeV). A precise determination of the electron and positron spectra and the temporal variation during

Table 1
Expected counts for all particle and average Jovian flux

$[E_1, E_2]$ (GeV)	N_{tot} (month^{-1})	N_J (month^{-1})	Min. sampl. time (months)	Percent. signal
0.05–0.07	10 ± 3	9 ± 3	1	90%
0.07–0.13	86 ± 9	12 ± 3	5	14%
0.13–0.60	$(220 \pm 1.5) \times 10^2$	(150 ± 12)	5	0.7%
0.60–2.0	$(339 \pm 1.8) \times 10^2$	(250 ± 16)	4	0.7%

The sampling time shows the minimum time required to get a signal at a 2σ level above galactic background assuming statistical errors.

recovery from the solar minimum will allow to gather information on solar modulation, also in respect to charge dependent effects reducing the systematics constraining propagation models in the galaxy and in the solar system. To determine the observational capabilities of PAMELA in the range 50 MeV–2 GeV we have divided (Casolino et al., 2008) the particle spectra in different ranges according to the spectral shape of galactic and Jovian electrons:

- 50–70 MeV: *non-reaccelerated component of Galactic and Jovian* e^-. The electrons in this range, at the lower limit of PAMELA detection capabilities, represent the primary non-reaccelerated component. These electrons are mostly of Jovian origin and do not undergo acceleration at the TS. Their long and short term modulation would give information on high energy acceleration phenomena in the Jovian magnetosphere and propagation effects in the inner heliosphere. As it is possible to see from Table 1, Jovian electrons are dominant in this energy range over galactic ones. In this way it is possible to measure the 13 month synodic period modulation with relative ease.
- 70–130 MeV: *accelerated component of Galactic* e^-*, primary Jovian* e^-. This is the highest energy electrons are believed to be accelerated by Jupiter. In this range Jovian flux is less abundant than Galactic one, but it will be possible to extract this signal thanks to the synodic modulation of the signal and determine the energy where the reaccelerated component starts to increase the flux.
- 130–600 MeV: *accelerated component of Galactic and Jovian* e^- *toward the maximum.* In this energy range Jovian electrons are reaccelerated at the TS. Their component is superimposed over the galactic flux.
- 600 MeV–2 GeV:*accelerated component of Galactic and Jovian* e^- *from the maximum.* These allows to gather a large number of events of electrons of Jovian origin in an energy range where they have never been observed. 2 GeV has been taken as the maximum detectable energy for accelerated protons according to Poitgieter and Ferreira (2002). In this and the former two cases it will be possible to extract the signal in the hypothesis of modulation of synodic year.

In Table 1 are shown the expected fluxes per month for the all particle cosmic rays and the average Jovian component. Aside from the 50–70 MeV range, where Jovian component is dominant, to separate the two components at higher energies it will be necessary to gather statistics over a time of the order of some months assuming that this signal will be modulated by Earth–Jupiter relative position.[2] It is possible to see how with PAMELA it will be possible to study for the first time the high energy Jovian electron component and test the hypothesis, the intensity of reacceleration at the solar wind Termination Shock (TS) and how this component is affected by the Earth–Jupiter synodic year.

6. Conclusions

In this work we have briefly described some of the observational possibilities of PAMELA in relation to solar and heliospheric physics. This will be the first time a magnetic spectrometer telescope in low Earth orbit will be operational for long duration observation. It will thus be possible to perform direct measurements in an energy range and with a precision up to now never reached for direct observations.

References

Adriani, O., Bonechi, L., Bongi, M. The magnetic spectrometer of the PAMELA satellite experiment. Nucl. Instr. Meth. Phys. Res. A 511, 72–75, 2002.

Barbarino, G.C., Boscherini, M., Campana, D., et al. The PAMELA time-of-flight system: status report. Nucl. Phys. (Proc. Suppl.) B 125, 298–302, 2003.

Bazilevskaya, G.A., Svirzhevskaya, A.K. On the stratospheric measurements of cosmic rays. Space Sci. Rev. 85, 431–521, 1998.

Boezio, M., Carlson, P., Francke, T., et al. The cosmic-ray electron and positron spectra measured at 1 AU during solar minimum activity. Astrophys. J. 532, 653–669, 2000.

Boezio, M., Bonvicini, V., Mocchiutti, E., et al. A high granularity imaging calorimeter for cosmic-ray physics. Nucl. Instr. Meth. Phys. Res. A 487, 407–422, 2002.

Casolino, M., Altamura, F., Basili, A. The PAMELA Storage and control unit. Adv. Space Res. 37 (10), 1857–1861, 2006.

Casolino, M., Picozza, P., Altamura, F., et al. Launch of the space experiment PAMELA. Adv. Space Res., in press, doi:10.1016/j.asr.2007.07.023.

Casolino, M., Di Felice, V., Picozza, P. Detection of the high energy component of Jovian electrons at 1 AU with the PAMELA experiment. Adv. Space Res. 41, 168–173, 2008.

Chenette, D.L. The propagation of Jovian electrons to earth. J. Geophys. Res. 85, 2243–2256, 1980.

Chupp, E.L., Forrest, D.J., Ryan, J.M., et al. A direct observation of solar neutrons following the 0118 UT flare on 1980 June 21. Astrophys. J. 263, L95–L99, 1982.

Eraker, J.H. Origins of the low-energy relativistic interplanetary electrons. Astrophys. J. 257, 862–880, 1982.

Evenson, P., Garcia-Munoz, M., Meyer, P. A quantitative test of solar modulation theory – The proton, helium, and electron spectra from 1965 through 1979. Astrophys. J. 275, L15–L18, 1983.

Ferreira, S.E.S., Potgieter, M.S., Burger, R.A., Heber, B., Fichtner, H. Modulation of Jovian and galactic electrons in the heliosphere 1.

[2] The two signals can also be separated using the maximum likelihood method assuming a sinusoidal signal with 13 months periodicity.

Latitudinal transport of a few MeV electrons. J. Geophys. Res. 106 (A11), 24979–24987, 2001.

Ferreira, S.E.S. The transport of galactic and Jovian cosmic ray electrons in the heliosphere. Adv. Space Res. 35, 586–596, 2005.

Gaffey, J., Bilitza, D. NASA/National Space Science Data Center trapped radiation models. J. Spacecraft Rockets 31 (2), 172–176, 1994 modelweb.gsfc.nasa.gov/magnetos/aeap.html, 1994.

Galper, A.M. Measurement of primary protons and electrons in the energy range of 10^{11}–10^{13} eV in the PAMELA experiment, in: Proceeding of the 27th ICRC, 2219–2222, Hamburg, 2001.

Leske, R.A., Mewaldt, R.A., Stone, E.C., et al. Observations of geomagnetic cutoff variations during solar energetic particle events and implications for the radiation environment at the Space Station. J. Geophys. Res. A 12, 30011–30022, 2001.

L'Heureux, J., Meyer, P. Quiet-time increase of low energy electrons: the Jovian origin. J. Astrophys. 209, 955–960, 1976.

Miroshnichenko, L. Solar Cosmic Rays. Kluwer, 2001.

Ogliore, R.C., Mewaldt, R.A., Leske, R.A., et al. A direct measurement of the geomagnetic cutoff for cosmic rays at space station latitudes, in: Proceeding of the 27th ICRC, 4112–4115, Hamburg, 2001.

Orsi, S., Carlson, P., Lund, J., et al. The anticoincidence shield of the PAMELA space experiment. Adv. Space Res. 37 (10), 1853–1856, 2006.

Picozza, P. et al. PAMELA – A Payload for Antimatter Matter Exploration and Light-nuclei Astrophysics. Astrop. Phys. 27 (4), 296, 2007.

Poitgieter, M.S., Ferreira, S.E.S. Effects of the solar wind termination shock on the modulation of Jovian and galactic electrons in the heliosphere. J. Geophys. Res. A 7, SSH 1, 2002.

Reames, D.V. Particle acceleration at the Sun and in the heliosphere. Space Sci. Rev. 90, 413–491, 1999.

Ryan, J.M. Long-duration solar gamma-ray flares. Space Sci. Rev. 93, 581–610, 2000.

Ryan, J.M. Solar Emissions, Rapp. Talk, 29th International Cosmic Ray Conference, Pune, vol. 10, p. 357–366, 2005.

http://www.spenvis.oma.be.

Shea, M.A., Smart, D.F. Solar proton and GLE event frequency: 1955–2000, in: Proceeding of the 27th ICRC, 3401–3404 Hamburg, 2001.

Simpson, J.A., Hamilton, D., Lentz, G., et al. Protons and electrons in Jupiter's Magnetic Field: results from the University of Chicago Experiment on Pioneer 10. Science 4122, 306–309, 1974.